JOURNAL OF CATALYSIS **171,** 54–66 (1997)
ARTICLE NO. CA971771

Nitric Oxide Reduction with Methane over Pd/TiO_2 Catalysts

II. Isotopic Labeling Studies Using N-15, O-18, and C-13

Mahesh W. Kumthekar[1] and Umit S. Ozkan[2]

Department of Chemical Engineering, 140 W. 19th Avenue, The Ohio State University, Columbus, Ohio 43210

Received August 28, 1996; revised May 19, 1997; accepted June 4, 1997

Reduction of NO with methane was investigated over Pd/TiO_2 catalysts using isotopically labeled species. Steady-state as well as unsteady-state isotopic labeling studies have been performed using the switches $^{14}N^{16}O \to {}^{15}N^{18}O$, $^{16}O_2 \to {}^{18}O_2$, $CH_4 + {}^{15}NO + O_2 \to CH_4 + {}^{14}NO + O_2$, $CH_4 + {}^{15}NO + O_2 \to CH_4 + O_2$, $^{13}CH_4 \to NO$, $^{13}CH_4 + NO \to He$, $^{13}CH_4 + NO \to NO$, $^{13}CH_4 + NO + O_2 \to NO$, $^{13}CH_4 \to O_2$, $CH_4 + {}^{15}NO \to CH_4 + {}^{15}N^{18}O$, and $N_2O \to He$, which have given some important clues regarding the mechanistic aspects of the NO–CH_4 interaction. Based on these studies, it was concluded that N_2 is formed through direct participation of CH_4 whereas N_2O formation is mainly a result of NO decomposition reaction. It was also observed that at least three types of reactions occur simultaneously on the surface, namely NO + CH_4, CH_4 oxidation and NO decomposition. The extent of these reactions is determined by the oxidation state of palladium on the surface.

INTRODUCTION

NO_x reduction using hydrocarbons, especially lower alkanes, as reducing agents has been an important area of research. The interest in this area was generated after the breakthrough result of Iwamoto which indicated that Cu–ZSM-5 was active for NO decomposition (1). Based on this work, several other studies were conducted which indicated that NO reduction with hydrocarbons was possible (2–7). Methane, being one of the primary components (more than 85%) of natural gas obviously offers a very attractive alternative as a reducing agent.

Several catalysts have been investigated for NO_x reduction with methane (8–12). A brief review has been presented in our previous papers (13, 14). A good catalyst for NO_x reduction with methane should selectively reduce NO_x even in the presence of excess oxygen and should have high thermal and hydrothermal stability. In previous publications (13–16), we have reported use of palladium-based catalysts as a possible alternative for this reaction and have described the results from pre- and postreaction catalyst characterization and temperature-programmed reduction experiments, as well as reaction studies performed in the presence and in the absence of gas-phase oxygen over a Pd/TiO_2 catalyst. The main observations from these earlier studies were that it was possible to completely convert NO with methane with or without gas phase oxygen being present in the feed. We also concluded that NO–CH_4 reaction, direct NO composition, and direct methane combustion were likely to take place on the surface simultaneously and the extent of each reaction was a strong function of the oxidation state of Pd and of the reaction parameters. It was also concluded that metallic palladium sites were needed to selectively reduce NO to N_2 and the transition between the Pd and PdO phases was relatively easy and rapid under reaction conditions.

As a continuation of this study, in this article we report the findings from isotopic labeling experiments in NO/CH_4 reactions performed under both steady-state and transient conditions. Techniques that involve isotopic labeling experiments have been especially powerful in elucidating reaction networks and understanding mechanistic aspects of catalytic reactions (17–19). The use of such experiments in our earlier studies of various catalytic systems were reported previously (16, 20–23). In this study, reactants labeled with C-13, N-15, and O-18 were used to examine the NO–CH_4 interaction with the surface in the presence and in the absence of oxygen. Findings from this study were combined with previously reported results to discuss the reaction network and possible catalytic sites involved in the NO–CH_4 reaction.

EXPERIMENTAL

Catalyst Preparation

The catalyst used in this study was 2 wt% Pd/TiO_2 which was prepared using a wet impregnation technique.

---

[1] Present address: Advanced Engineering Group, IMPCO/Air Sensors, 16804 Gridley Place, Cerritos, CA 90703-1741.

[2] To whom correspondence should be addressed. E-mail: ozkan.1@osu.edu.

0021-9517/97 $25.00

The preparation has been described earlier (15). The TiO_2 (anatase) (Aldrich) support was wet impregnated with a solution of Pd-acetate (Aldrich). The solution was then stirred at 90°C for 4.5 hr followed by overnight drying of the slurry at 100°C. The resulting precursor was then calcined at 500°C for 5 hr in oxygen. The surface area of the catalysts used in this study was 12 m^2/g.

Isotopic Labeling Studies

The isotopic labeling techniques used in this study included both steady state and transient kinetic analysis methods. The first technique involves application of a step change to the system at steady state, where one feed stream is abruptly replaced by a feed stream in which one or more of the reactants are isotopes of their counterparts in the previous stream. The steady state is not perturbed during the step change and the transients of various isotopes (for both reactants and products) are continuously monitored by a mass spectrometer. The second transient technique used in this study involves abruptly removing one or more of the reactants from the feed stream after the steady state is established and letting the reaction subside at its own pace while simultaneously monitoring the decay profiles of various reactant and product species with a mass spectrometer. The specific interactions examined in this study are $NO{-}CH_4$ reaction in the presence and the absence of oxygen, NO/surface interaction, and O_2/surface interaction.

The reactor system used for the isotopic transient studies has been discussed in detail earlier (22, 23). It consists of a feed system with mass flow controllers (Tylan model FC-280), a fixed-bed reactor, and a gas chromatograph–mass spectrometer (Hewlett–Packard 5890 GC–Hewlett–Packard 5989A MS engine). The reaction experiments were carried out on a fixed bed of catalyst in a tubular reactor measuring 6.4 mm O.D. × 4.6 mm I.D. The catalyst loading was kept constant at 37.5 mg for different reactions. The effluent gases from the reactor were analyzed by bleeding a small amount through a blank capillary column into a gas chromatograph–mass spectrometer (GC–MS) (HP 5989 MS engine). The product analysis was also carried out by using an on-line GC and on-line chemiluminescence NO_x analyzer (Thermo Environmental Instruments, model 10). The reaction temperature was maintained at 500°C for all the reactions.

The transient analyses were carried out by allowing the reaction to reach steady-state and abruptly applying a step change to the system. The steady state was verified by the product profiles obtained from the mass spectrometer. The space velocity of the system was maintained at a constant level before and after the switch in all experiments. This was to ensure that the nature of the profiles obtained is a result of the reactions on the surface of the catalyst and not due to a change in flow rate. Additional helium was introduced to compensate for the amount of reactant which was removed from the feed stream in unsteady-state experiments. The concentrations of the gases during the isotopic switches were kept the same as those in the conventional steady state experiments. In nitric-oxide-exchange experiments the concentration of NO was maintained at 1780 ppm and in oxygen-exchange experiments the concentration was kept at 3800 ppm. In other isotopic-labeling studies methane concentration was always maintained at 2.13% ppm and NO concentration at 1780 ppm. Wherever oxygen is used, its concentration was maintained at 2100 ppm. For all the isotopic labeling experiments, the catalyst was prereduced in hydrogen *in situ* at 200°C for 30 min, followed by flushing with helium at 200°C for 1 hr unless otherwise stated. In general, the isotopic transients were monitored for at least 10 min following the switch. The transients are presented in the form of normalized concentrations of isotopes. In the case of steady-state experiments, the normalized concentrations are calculated such that the summation of all isotopes of a given species is unity. In the case of unsteady-state experiments, the normalized concentrations are calculated by taking the signal right before the switch as unity.

The following isotopic labeling experiments were performed to provide an understanding of the mechanistic aspects of these reactions: $Ar \rightarrow He$, $^{14}N^{16}O \rightarrow {}^{15}N^{18}O$ (with and without the prereduction step), $^{16}O_2 \rightarrow {}^{18}O_2$ (without the prereduction step), $CH_4 + {}^{15}NO + O_2 \rightarrow CH_4 + {}^{14}NO + O_2$, $CH_4 + {}^{15}NO + O_2 \rightarrow CH_4 + O_2$, $^{13}CH_4 \rightarrow NO$, $^{13}CH_4 + NO \rightarrow He$, $^{13}CH_4 + NO \rightarrow NO$, $^{13}CH_4 + NO + O_2 \rightarrow NO$, $^{13}CH_4 \rightarrow O_2$, $CH_4 + {}^{15}NO \rightarrow CH_4 + {}^{15}N^{18}O$, and $N_2O \rightarrow He$ (with and without the prereduction step).

RESULTS

Transient Analyses Using Isotopic Labeling

Dead time measurement. The isotopic labeling experiments are based on imposing a step function change to the system at steady state. The steady state of the system may or may not continue after the step function depending on the nature of the change imposed. The response of the system to this step change is monitored as a function of time by a mass spectrometer. The dead time of the fixed bed of catalyst used in these experiments is measured by switching a steady Ar flow to helium in the same way as was done for all the step changes imposed. The decay of the Ar curve through a fixed bed of catalyst is shown in Fig. 1a. It is seen that in about a minute all the Ar is flushed out of the system.

Oxygen exchange characteristics of the catalyst surface. The oxygen exchange characteristics of the catalyst surface were investigated with a $^{16}O_2 \rightarrow {}^{18}O_2$ switch. The oxygen transients in the absence of the reactant gases over oxidized Pd/titania within the first 5 min of the switch are plotted in

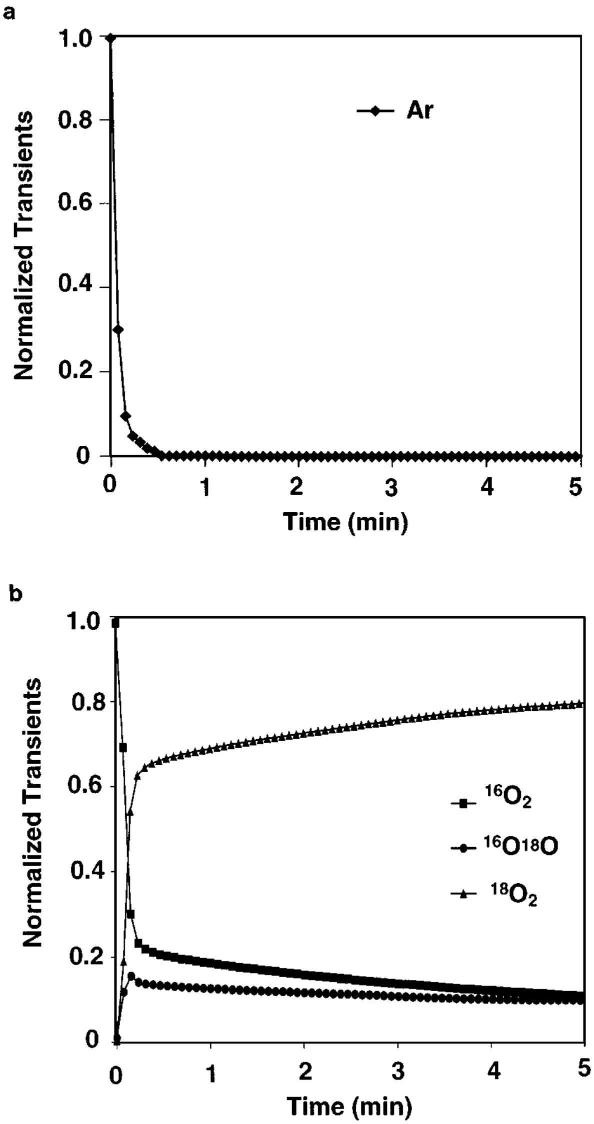

FIG. 1. Normalized transients in (a) Ar → He and (b) $^{16}O_2 \rightarrow {}^{18}O_2$ switches.

Fig. 1b. This switch was performed at 500°C at an oxygen concentration of 3800 ppm. The most interesting feature observed was the presence of cross-labeled oxygen $^{16}O^{18}O$ which signifies the product of a so-called scrambling process between the gas phase oxygen and surface oxygen. Another interesting feature observed is the presence of an $^{16}O_2$ signal that continues for several minutes after the inlet $^{16}O_2$ is substituted with $^{18}O_2$ through the switch. The $^{16}O^{18}O$ as well as $^{16}O_2$ signals remained at a nonzero value for a fairly long time after the switch, indicating a steady participation of the lattice oxygen in the exchange processes. The $^{18}O_2$ signals rose immediately to an intermediate value and then slowly approached the inlet value.

A similar $^{16}O_2 \rightarrow {}^{18}O_2$ switching experiment performed in an empty reactor to examine the homogeneous oxygen scrambling and/or oxygen exchange with the reactor walls showed immediate rise and decline of $^{18}O_2$ and $^{16}O_2$ signals, respectively, with no cross-labeled oxygen being formed, eliminating any possibility of homogeneous oxygen exchange under the reaction conditions employed.

The oxygen exchange characteristics of the catalyst surface with a nitric oxide molecule were also investigated by switching from $^{14}N^{16}O$ to $^{15}N^{18}O$ at 500°C. The concentration of nitric oxide in this experiment before and after the switch was maintained at 1780 ppm. The transient curves of nitric oxide isotopes obtained over an oxidized catalyst are illustrated in Fig. 2a. One of the important observations in this experiment was a sharp rise in the $^{15}N^{16}O$ signal immediately after the switch, followed by a slow decay with time,

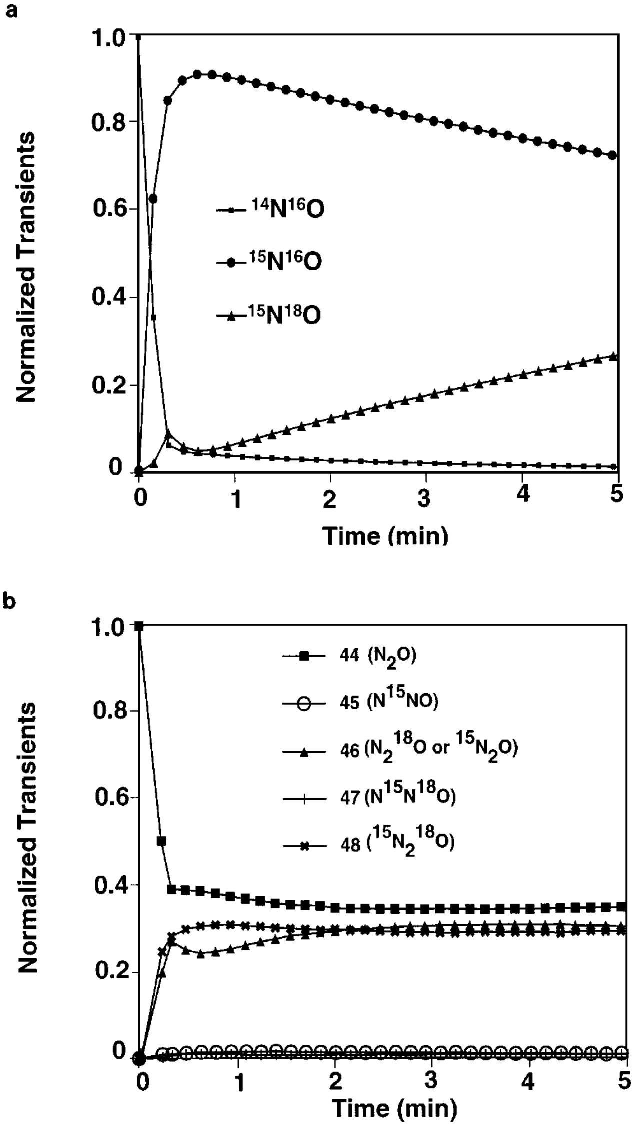

FIG. 2. Normalized transients in $^{14}N^{16}O \rightarrow {}^{15}N^{18}O$ switch over oxidized Pd/TiO$_2$ (a) nitric oxide isotopes or (b) nitrous oxide isotopes.

indicating substantial oxygen exchange between the catalyst surface and the nitric oxide molecule. Even 10 min after the switch, 55% of the nitric oxide coming out of the reactor was still $^{15}N^{16}O$. Similarly, the normalized $^{15}N^{18}O$ signal did not rise to unity immediately. Instead it increased slowly, approaching the inlet value. It was also observed that the signal for $^{14}N^{16}O$ declined very fast and went down to a value close to zero almost immediately after the switch.

The most striking feature in this experiment was the formation of various isotopes of nitrous oxide. This is significant in showing that the oxidized catalyst surface is capable of combining two NO molecules to give a N_2O molecule. The profiles of these isotopes are shown in Fig. 2b. The transient for $m/e = 44$ representing $^{14}N_2O$ was seen to have a slow relaxation, staying at around 40% even 5 min after the switch. The profiles of $m/e = 45$ and 47 represent $N^{15}NO$ and $N^{15}N^{18}O$, respectively, and were zero throughout the experiment. This indicates that there is no cross-labeling in the nitrous oxide molecules with respect to the two nitrogen atoms. The profile of $m/e = 46$ showed a steady value of around 30% of the total nitrous oxide produced. This signal could either represent $N_2{}^{18}O$ or $^{15}N_2O$. Under the present isotopic labeling scheme it was not possible to distinguish between these two species. There is also the possibility that the $m/e = 46$ signal could be due to $^{14}N^{16}O_2$ produced from the $3NO \rightarrow N_2O + NO_2$ reaction. However, if there were nitrogen dioxide forming in this experiment, we would expect to see some additional isotopes such as $^{15}NO^{16}O^{18}O$ or $^{15}N^{18}O_2$. The fact that there was no signal for $m/e = 49$ or 50 leads us to safely exclude nitrogen dioxide formation. The profile for $m/e = 48$ which represented $^{15}N_2{}^{18}O$ was still around 30% at the end of 5 min after the switch.

A similar NO exchange experiment was performed over a prereduced Pd/titania catalyst by switching from $^{14}N^{16}O$ to $^{15}N^{18}O$. The transients of the three isotopes of nitric oxide are shown in Fig. 3a. The most important finding in this experiment was that the NO molecule was capable of exchanging its oxygen even with the reduced catalyst. Similar to the experiment on an untreated catalyst, a sharp rise in the $^{15}N^{16}O$ signal followed by a slow decay with time was observed. The normalized $^{15}N^{18}O$ signal did not rise to unity immediately. Instead it increased slowly in approaching the inlet value. This indicated substantial oxygen exchange between the reduced catalyst surface and the incoming nitric oxide molecules. Even 10 min after the switch, 32% of the nitric oxide coming out of the reactor was still $^{15}N^{16}O$. The $^{14}N^{16}O$ signal relaxed to zero essentially in the same time frame as the inert after the switch. In this experiment, the behavior in the initial few minutes after the switch is representative of the reduced catalyst, while as time proceeds, the behavior observed becomes that of a slowly oxidizing catalyst through the oxygen from the nitric oxide molecule.

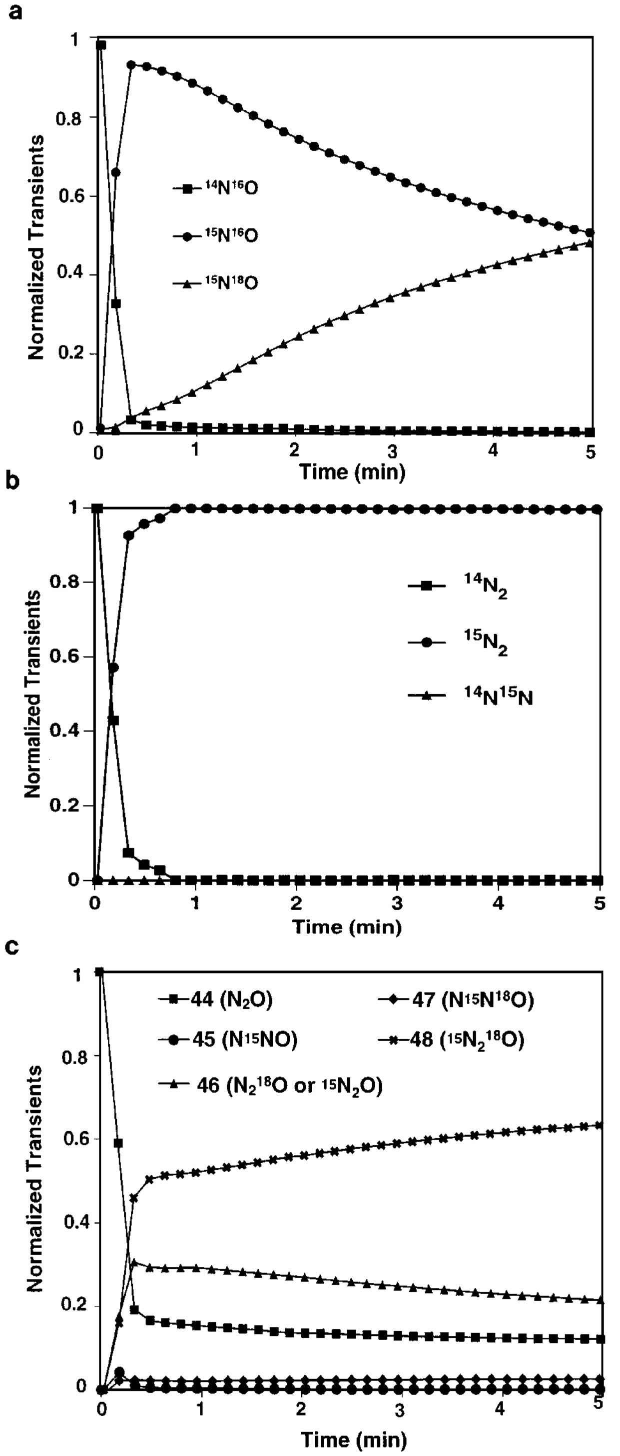

FIG. 3. Normalized transients in $^{14}N^{16}O \rightarrow {}^{15}N^{18}O$ switch over prereduced Pd/TiO$_2$ (a) nitric oxide isotopes, (b) nitrogen isotopes, or (c) nitrous oxide isotopes.

As expected, nitric oxide decomposition reaction was observed over the prereduced catalyst. Nitrous oxide and nitrogen were the two products formed. The transients for the various isotopes of nitrogen are shown in Fig. 3b. A very sharp decline in $^{14}N_2$ was observed, indicating that neither the nitrogen molecule nor an intermediate that leads to

N_2 lingers on the surface for any appreciable amount of time. Correspondingly, the normalized response of doubly labeled nitrogen, i.e., $^{15}N_2$, rose to unity very quickly. Another important observation was that there was no cross-labeled nitrogen, i.e., $^{14}N^{15}N$, observed throughout the experiment.

The transients of nitrous oxide isotopes are presented in Fig. 3c. The profiles of these isotopes are quite similar to what has been observed over the oxidized catalysts, in that there is no cross-labeled species ($N^{15}NO$ or $N^{15}N^{18}O$) observed and that the doubly unlabeled nitrous oxide ($m/e = 44$) signal does not relax to zero during the 10 min in which the transient has been monitored. However, the normalized concentration at the end of 5 min (∼20%) is considerably lower than what was observed over the oxidized sample at the same time (∼40%).

Transients of N-containing species. NO reduction reaction with methane was investigated over Pd/TiO_2 catalyst by following transients of N-containing products, i.e., N_2 and N_2O, in different switches. Step-function changes were applied under both steady state and unsteady state conditions. The isotopic switch used to follow the nitrogen and nitrous-oxide transients under steady state conditions was $CH_4 + {}^{15}NO + O_2 \rightarrow CH_4 + {}^{14}NO + O_2$. The reaction was performed at 500°C with an oxygen concentration of 2100 ppm. The transients of nitrogen isotopes are presented in Fig. 4a. It was seen that the doubly labeled nitrogen, i.e., $^{15}N_2$, signal fell down to zero immediately after the switch. The signal for doubly unlabeled nitrogen, i.e., $^{14}N_2$, correspondingly went to a normalized value of unity immediately. Another important observation to note was the absence of cross-labeled nitrogen, i.e., $^{14}N^{15}N$.

The relaxation profiles for nitrous oxide isotopes in the first 5 min after the switch are presented in Fig. 4b. It is important to note that the normalized transients for doubly labeled nitrous oxide, i.e., $^{15}N_2O$, showed a very slow relaxation after the gas phase nitric oxide was switched from ^{14}NO to ^{15}NO. In fact, 5 min after the switch 30% of the nitrous oxide coming out of the reactor was still doubly labeled. Similar to the nitrogen transients, there was no cross-labeled nitrous oxide, i.e., $^{14}N^{15}NO$, observed in this experiment. The delayed relaxation of the transients for nitrous oxide suggests that the intermediates leading to its formation have a substantially longer surface residence time, especially when compared to that of the N_2 transients.

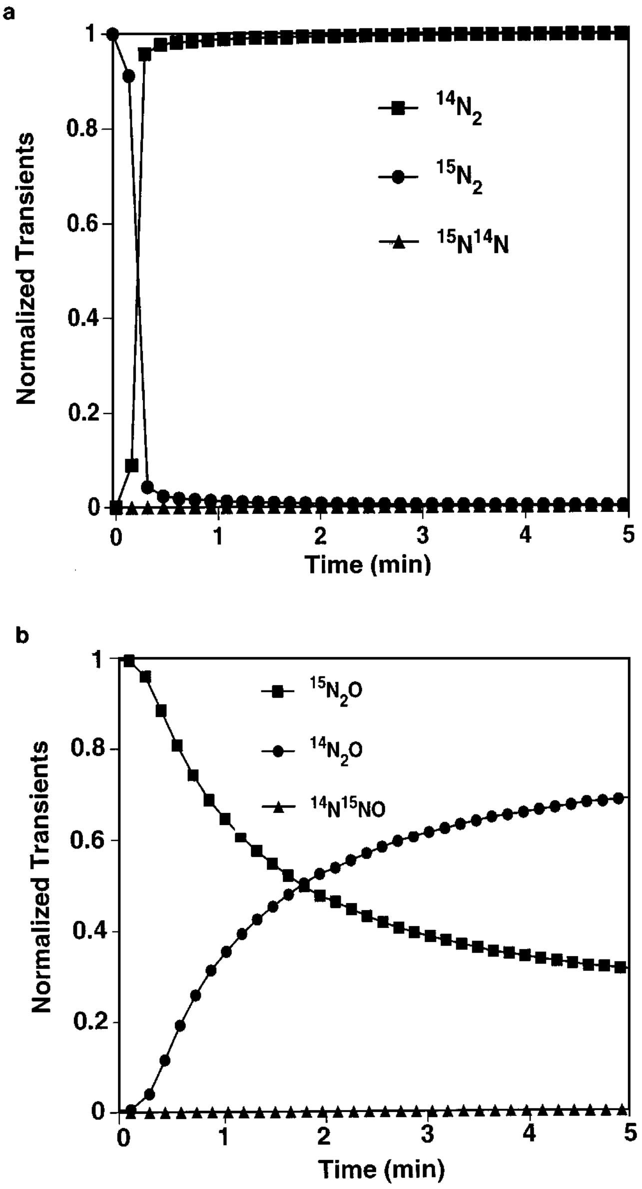

FIG. 4. Normalized transients in $CH_4 + {}^{15}NO + O_2 \rightarrow CH_4 + {}^{14}NO + O_2$ switch (a) nitrogen isotopes or (b) nitrous oxide isotopes.

One of the step-function changes imposed on the system without maintaining the steady state was a switch from $CH_4 + {}^{15}NO + O_2 \rightarrow CH_4 + O_2$. This experiment was performed at 500°C with an oxygen concentration of 2100 ppm. In this case, the flow of ^{15}NO to the reactor was discontinued abruptly (by replacing it with an equal amount of helium so that the space velocity of the system did not change before or after the switch) and the reaction was allowed to subside at its own pace. The nitrogen ($^{15}N_2$) and nitrous oxide ($^{15}N_2O$) transients are plotted in Fig. 5. It can be clearly seen that the $^{15}N_2O$ transients relax much more slowly as compared to the $^{15}N_2$ transients, agreeing with the earlier results.

Another unsteady-state experiment performed to provide an understanding of the differences between the formation routes of N_2 and N_2O was $^{13}CH_4 \rightarrow NO$. In this experiment, C-13-labeled methane was used to differentiate between CO and N_2 signals and CO_2 and N_2O signals. Before the switch, the prereduced catalyst was saturated with $^{13}CH_4$ (2.12% in He) at 500°C for 30 min. Then the methane flow was discontinued abruptly and was replaced with an NO flow (1780 ppm in He). The formation of N_2 and N_2O

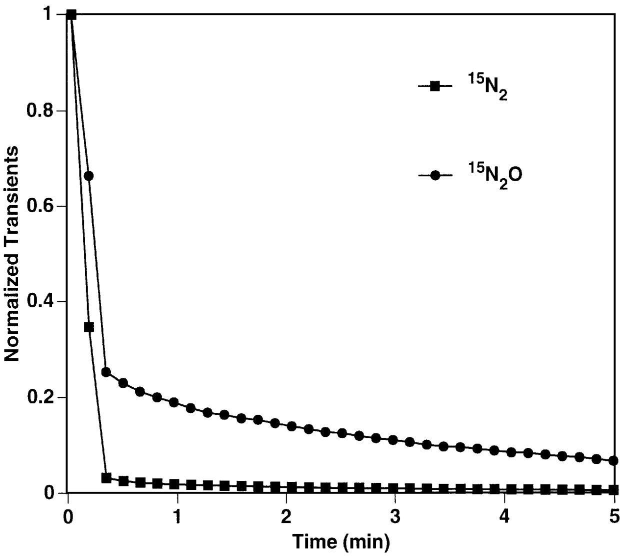

FIG. 5. Normalized transients of nitrogen and nitrous oxide isotopes in $CH_4 + {}^{15}NO + O_2 \rightarrow CH_4 + O_2$ switch.

was monitored as a function of time. The profiles for these products are presented in Fig. 6. It can be very clearly seen that N_2O formation lags behind N_2 formation by 0.079 min. The delay in the formation of N_2O as compared to N_2 complements the data from the earlier experiments in suggesting that the formation routes for these two products are different and that the intermediates leading to N_2O formation have a longer surface life as compared to those leading to N_2 formation.

Transients for N_2 and N_2O were also monitored in unsteady-state experiments where methane was cut off and the reaction was allowed to subside. The switches performed in the presence as well as in the absence of oxygen were ${}^{13}CH_4 + NO + O_2 \rightarrow NO + O_2$ and ${}^{13}CH_4 + NO \rightarrow NO$.

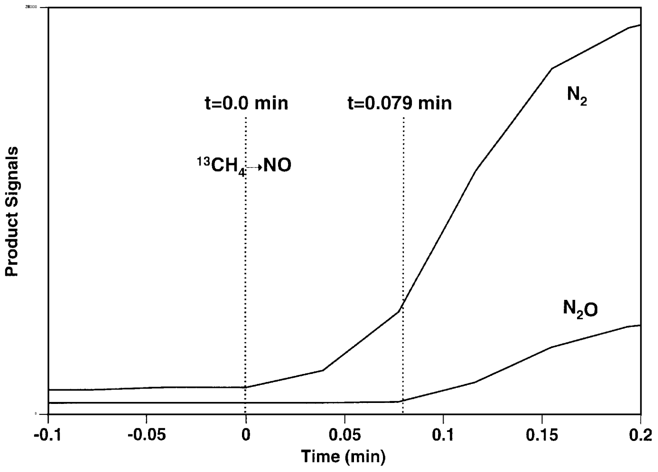

FIG. 6. Product signals for N_2 and N_2O in ${}^{13}CH_4 \rightarrow NO$ switch.

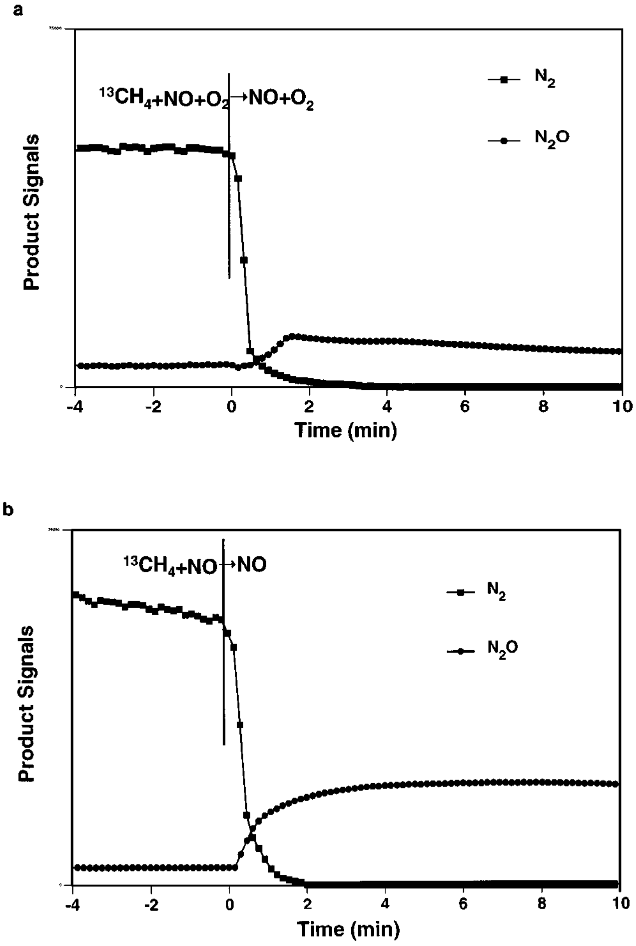

FIG. 7. Product signals for N_2 and N_2O in (a) ${}^{13}CH_4 + NO + O_2 \rightarrow NO + O_2$ switch and in (b) ${}^{13}CH_4 + NO \rightarrow NO$ switch.

As expected, the N_2 transients went down sharply after the switch in both experiments (Fig. 7). The N_2O signal, on the other hand, showed a pronounced rise, suggesting that the primary product from NO–CH_4 interaction is nitrogen and that the nitrous oxide formation is mainly the result of direct NO decomposition. The gradual rise in the N_2O signal is also consistent with our previous results which suggested dimerized intermediates with longer surface residence times leading to N_2O formation.

Transients for carbon oxides. NO–CH_4 interaction as well as CH_4/surface interaction were examined by following the transients of carbon oxides over Pd/TiO_2 catalyst. The switches performed were ${}^{13}CH_4 + NO \rightarrow He$, ${}^{13}CH_4 + NO \rightarrow NO$, ${}^{13}CH_4 + NO + O_2 \rightarrow NO$, and ${}^{13}CH_4 \rightarrow O_2$. These experiments were performed over prereduced catalysts at 500°C and using NO, CH_4, and O_2 concentrations of 1780 ppm, 2.12%, and 2100 ppm, respectively. In the fourth switch the reduced surface was saturated with ${}^{13}CH_4$ at 500°C.

The transients obtained for ${}^{13}CO$ and ${}^{13}CO_2$ in ${}^{13}CH_4 + NO \rightarrow He$ switch are presented in Fig. 8a. It can clearly

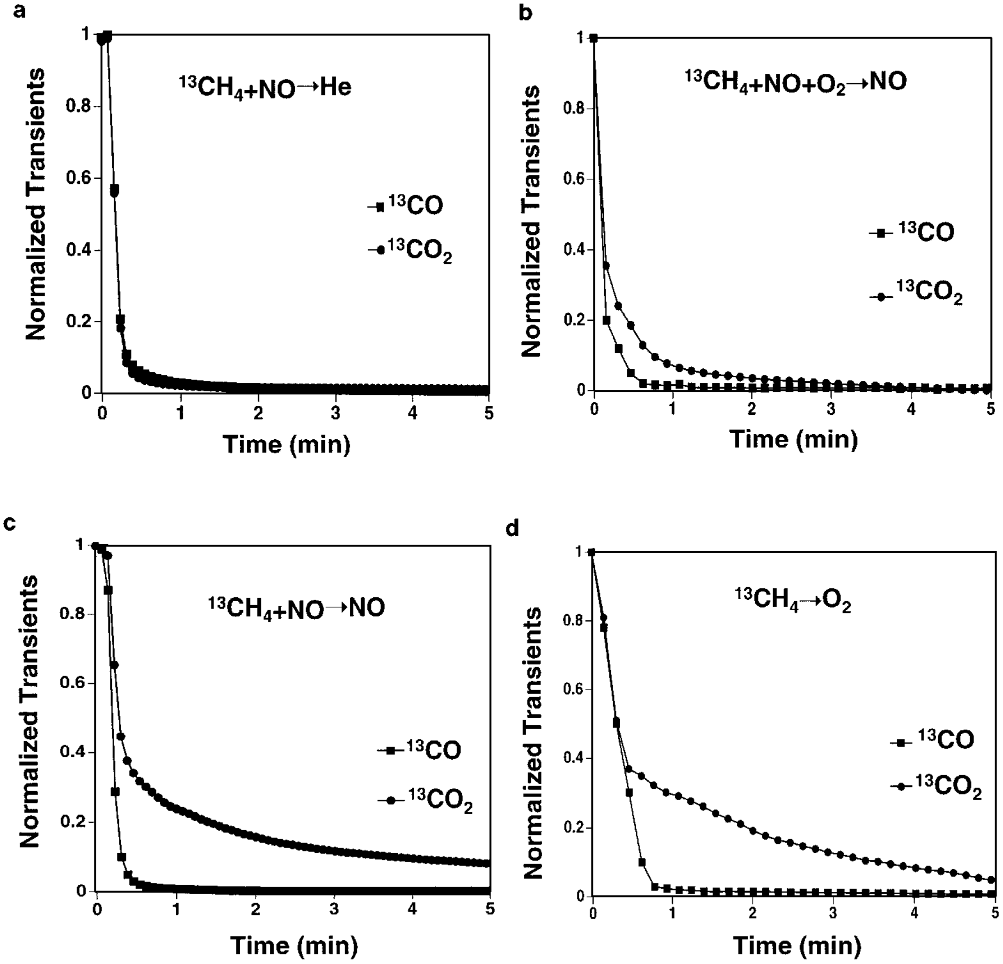

FIG. 8. Normalized transients for carbon oxides in (a) $^{13}CH_4 + NO \rightarrow$ He switch, in (b) $^{13}CH_4 + NO + O_2 \rightarrow NO$ switch, in (c) $^{13}CH_4 + NO \rightarrow NO$ switch, and in (d) $^{13}CH_4 \rightarrow O_2$ switch.

be seen that both ^{13}CO and $^{13}CO_2$ transients relax to zero very fast after the switch. In the second experiment performed where the $^{13}CH_4 + NO + O_2$ stream was switched to NO, the $^{13}CO_2$ transient was seen to relax more slowly than ^{13}CO, as shown in Fig. 8b. In the third experiment where the $^{13}CH_4 + NO$ stream was switched to NO, the decay profiles were similar to what was seen in the previous experiment, with the $^{13}CO_2$ signal having a much slower decay rate than ^{13}CO (Fig. 8c). When similar transients were followed during $^{13}CH_4 \rightarrow O_2$, the rate at which the $^{13}CO_2$ transient relaxed to zero was even slower, with the normalized concentration staying at nonzero value even at the end of the fifth minute after the switch (Fig. 8d).

Another interesting experiment performed was the switch from $CH_4 + {}^{15}NO$ to $CH_4 + {}^{15}N^{18}O$. The purpose of this experiment was to examine the origin of the oxygen incorporated into CO or CO_2 molecules. Three different isotopes of carbon dioxide were observed, namely, $C^{16}O_2$, $C^{16}O^{18}O$, and $C^{18}O_2$. The profiles observed for these CO and CO_2 isotopes are compared in Fig. 9. The relaxation of O-16 containing isotopes was seen to be much faster in the case of carbon monoxide than it was for carbon dioxide.

DISCUSSION

In our previous article (14) we reported that, following the prereduction step, the palladium on the titania surface is primarily in metallic form. In the temperature-programmed studies performed over these catalysts (13), it was observed that deposition of Pd on the titania surface made the titania support more readily reducible. In agreement with earlier reports in the literature (24–27), the oxygen from the titania lattice was considered to become more accessible after the Pd deposition, and a partial reoxidation of the palladium by oxygen diffusing from the titania support was reported as a possibility. Also reported in the previous article was a multireaction scheme, which included $NO-CH_4$ interaction, direct NO decomposition, and direct CH_4 combustion. The extent of each of these reactions appeared to be determined by the state of the palladium (the oxidic or the

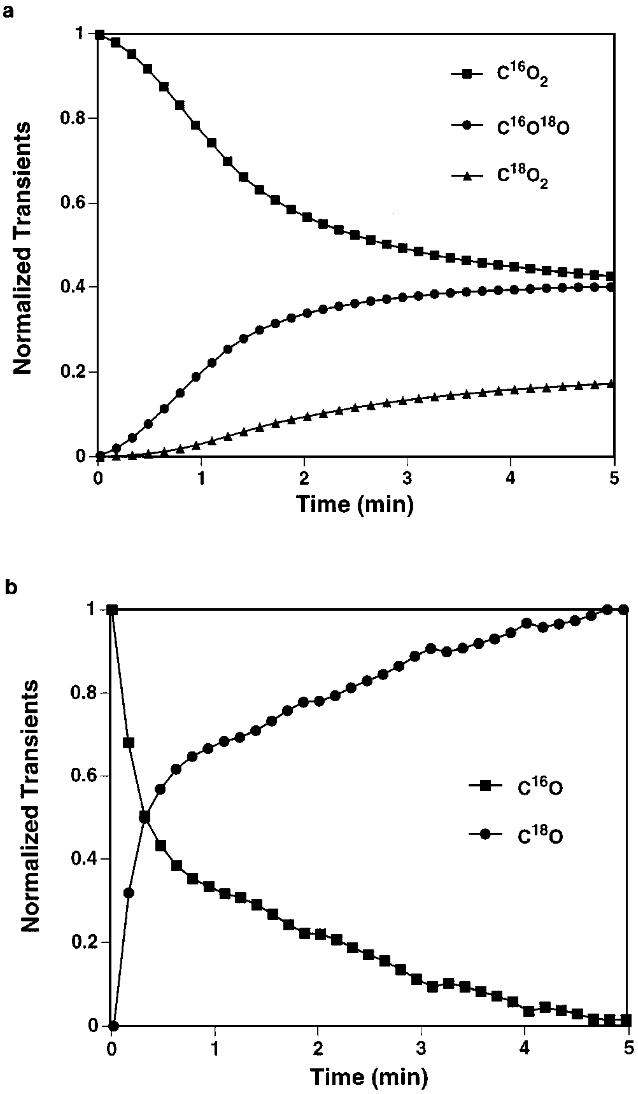

FIG. 9. Normalized transients in $CH_4 + {}^{15}N^{16}O \rightarrow CH_4 + {}^{15}N^{18}O$ switch (a) carbon dioxide isotopes and (b) carbon monoxide isotopes.

metallic phase) on the surface, which in turn could transform very rapidly depending on the reaction media. In this article, we examine the results of isotopic labeling studies and discuss these findings in terms of our previous observations reported in earlier articles (13, 14).

Oxygen Exchange Characteristics of Pd/Titania Catalysts

One of the important findings of this study was the ability of the catalyst surface to exchange its oxygen with gas phase NO as well as O_2 molecules, as demonstrated by the step function changes of ${}^{16}O_2 \rightarrow {}^{18}O_2$ and ${}^{14}N^{16}O_2 \rightarrow {}^{15}N^{18}O_2$. Similar switches performed in an empty reactor did not show any gas phase scrambling or any interaction with the reactor walls. The transients for unlabeled species relaxed to zero within the gas-phase hold-up time.

The oxygen exchange experiments with molecular oxygen over the oxidized Pd/titania catalyst showed the formation of cross-labeled oxygen, ${}^{16}O^{18}O$, in addition to a slow decaying profile for ${}^{16}O_2$ (Fig. 1b). The mechanism of the exchange of gas-phase oxygen with the lattice oxygen has been studied extensively by Winter (28) over several oxides. The presence of ${}^{16}O$ in the gas phase several minutes after the switch indicates the accessibility of lattice oxygen for exchange. At the end of 10 min, about 20% of the oxygen in the gas phase remained unlabeled. The presence of both cross-labeled oxygen, ${}^{16}O^{18}O$, and doubly unlabeled oxygen, ${}^{16}O_2$, in these experiments right from the beginning suggests that over this catalyst the exchange takes place through both a “four-atom complex” and a “three-atom complex” as suggested by Winter (28). This finding could also suggest the presence of two different sites for oxygen exchange.

The Pd/TiO$_2$ catalyst was also seen to be active in exchanging its oxygen with the gas phase nitric oxide molecules. When the NO exchange experiment was performed over the fresh catalyst (oxidized) the interaction appeared to be fast, leading to more than 90% of the incoming NO molecules exchanging their oxygen upon contact with the catalyst surface, as seen by the immediate rise in ${}^{15}N^{16}O$ signal (Fig. 2a). Similar exchange phenomena have been reported earlier over various metal oxides (22, 23, 28–31). Shelef has reported an entire oxygen monolayer and even some subsurface oxygen being exchanged at higher temperatures (29) in some cases and has suggested that nitrite ions or nitro complexes serve as surface intermediates during the exchange.

An interesting finding of these studies is that the oxygen exchange experiments with both O_2 and NO showed that the total oxygen exchanged in the first 5 min after the switch was significantly larger than the amount of oxygen present in PdO over the catalyst. At the end of 5 min, the total amount of oxygen atoms exchanged in the form of both ${}^{16}O^{18}O$ and ${}^{16}O_2$ was 18.9 μmol/m^2 for the ${}^{16}O_2 \rightarrow {}^{18}O_2$ experiment. The corresponding value for the $NO \rightarrow {}^{15}N^{18}O$ experiment was 20.3 μmol/m^2. At the end of 10 min, these values were 30.0 and 35.7 μmol/m^2, respectively. The fact that these values are considerably greater than the total amount of oxygen present in the form of PdO (15.6 μmol/m^2) shows that not only oxygen in the PdO phase is readily available for exchange, but also the oxygen in the PdO–TiO$_2$ interface or even in the TiO$_2$ bulk is accessible. Although our earlier studies (30, 31) have shown oxygen exchange of NO over the bare TiO$_2$ support (24 μmol/m^2 at the end of 12 min), we suspect that the presence of Pd may have enhanced the exchange capability.

When a similar NO exchange experiment was performed over a prereduced catalyst it was observed that even the reduced catalyst was capable of exchanging oxygen with incoming NO molecules (Fig. 3a). Whether part of this exchange is due to a partial reoxidation of the Pd with oxygen diffusing from the support is not clear. However, the controlled-atmosphere XPS studies (13) which showed the presence of PdO in the prereduced catalyst suggests that the partial reoxidation of the metal due to the increased oxygen mobility of titania as a result of palladium loading is a strong possibility.

Interaction of NO with Pd/TiO$_2$ Surfaces

The interaction of nitric oxide with various noble metals, including Pd-based catalysts (32–34), has been a topic of intense research mainly because of the environmental issues concerning NO_x and the use of noble metals in the automobile converters.

Our previous temperature-programmed desorption studies performed over prereduced Pd–titania catalysts indicated the presence of two types of sites available for NO adsorption (13). Out of these two, the stronger site was shown to lead to the formation of a N_2O molecule. Isotopic labeling studies performed at steady-state and at transient conditions provided further clues regarding the interaction of NO with Pd/TiO$_2$ surfaces. The $^{14}N^{16}O \rightarrow {}^{15}N^{18}O$ step function change performed in order to examine the oxygen exchange characteristics of the catalyst surface showed the formation of nitrous oxide over freshly oxidized catalyst (Fig. 2b). Interestingly, there was no nitrogen formation over this catalyst. This experiment showed that the oxidized catalyst at 500°C is capable of coupling two NO molecules to give a N_2O molecule, independent of the presence of methane or any other reducing agent. Equally important as this observation was the fact that the transient for N-14 labeled nitrous oxide showed a very slow decay behavior, suggesting a long-surface life for the intermediate leading to N_2O formation. Also, the facts that the N-14 labeled nitric oxide transient decayed much faster and that there was no cross-labeled nitrous oxide species, i.e., $^{14}N^{15}NO$, point to an intermediate that already has undergone a coupling step. Combining this observation with the results from our NO temperature-programmed desorption experiments (13) and some earlier reports in the literature, it is envisioned that a stable, dimer-type species acts as an intermediate for the N_2O formation in direct decomposition of NO.

A similar switch from unlabeled NO to labeled $^{15}N^{18}O$ over a prereduced catalyst also showed the presence of N_2O. The main difference between the two experiments was the formation of nitrogen over the prereduced catalyst which was not seen over the fresh catalyst. While the nitrous oxide transients over the prereduced catalysts (Fig. 3c) showed behavior very similar to that observed over the oxidized catalyst, with slow decay of the $^{14}N_2O$ signal and no formation of cross-labeled species, nitrogen transients (3b) behaved very differently, with the $^{14}N_2$ signal decaying to zero within the gas-phase hold-up time. Based on this observation, it appears that NO decomposition to N_2 can only take place over completely reduced catalyst, while N_2O formation proceeds over reduced as well as over oxidized catalysts. It also appears that the formation routes and/or intermediates for these two products are completely different.

These suggestions are further supported by isotopic labeling experiments involving both NO and CH_4 (and in some cases oxygen) in the feed stream. The step function change $CH_4 + {}^{15}NO + O_2 \rightarrow CH_4 + {}^{14}NO + O_2$ applied to a prereduced catalyst without perturbing the steady state showed major differences in the decay profiles of the doubly-labeled nitrogen and doubly-labeled nitrous oxide profiles (Figs. 4a and 4b). While the $^{15}N_2$ transient relaxed to zero within the gas-phase hold-up time, the $^{15}N_2O$ transient showed a very slow decline. There were no cross-labeled isotopes for either species. These results also show two different formation routes for N_2 and N_2O under steady-state conditions of $NO + CH_4 + O_2$ reaction. Another experiment that reiterated this finding was performed by replacing NO with He through the $CH_4 + {}^{15}NO + O_2 \rightarrow CH_4 + He + O_2$ switch. The transients for $^{15}N_2$ and $^{15}N_2O$ are presented in Fig. 5, and exhibit very similar decay behavior for the two species to that observed in the other isotopic labeling experiments, again showing a much slower decline in the $^{15}N_2O$ signal.

Another transient experiment which involved the $^{13}CH_4 \rightarrow NO$ switch showed the initial relative rates of N_2 and N_2O formation (Fig. 6). The nitrogen signal started rising within the gas-phase hold-up time, probably due to the interaction of incoming NO with the CH_x species which were left on the surface from the methane flow. It took 0.079 min longer for the N_2O signal to start increasing above the background level, suggesting a difference in the life spans of intermediates leading to N_2 versus those leading to N_2O formation. Another possible explanation for this observation is that N_2 is formed primarily on the reduced Pd sites and N_2O is formed on oxidized Pd sites. As the catalyst becomes oxidized through the nitric oxide decomposition reaction, we start observing N_2O formation.

When other transient experiments were performed by cutting off the methane stream, as in the switches $^{13}CH_4 + NO \rightarrow NO$ and $^{13}CH_4 + NO + O_2 \rightarrow NO + O_2$, the nitrogen signal showed a drop to the background level within 2 min after the switch, the amount of time needed for the CH_x species on the surface to be depleted by interaction with NO (Fig. 7). The N_2O signal, on the other hand, had a pronounced increase after the switch, and stayed at that level for the 15 min during which the transients were monitored, indicating that in the absence of methane NO decomposition to N_2O is the dominant reaction and can be sustained for a long time. The fact that the rise to the postswitch steady-state value was relatively small was in complete agreement with our previous observations that showed a longer surface life for the N_2O intermediates.

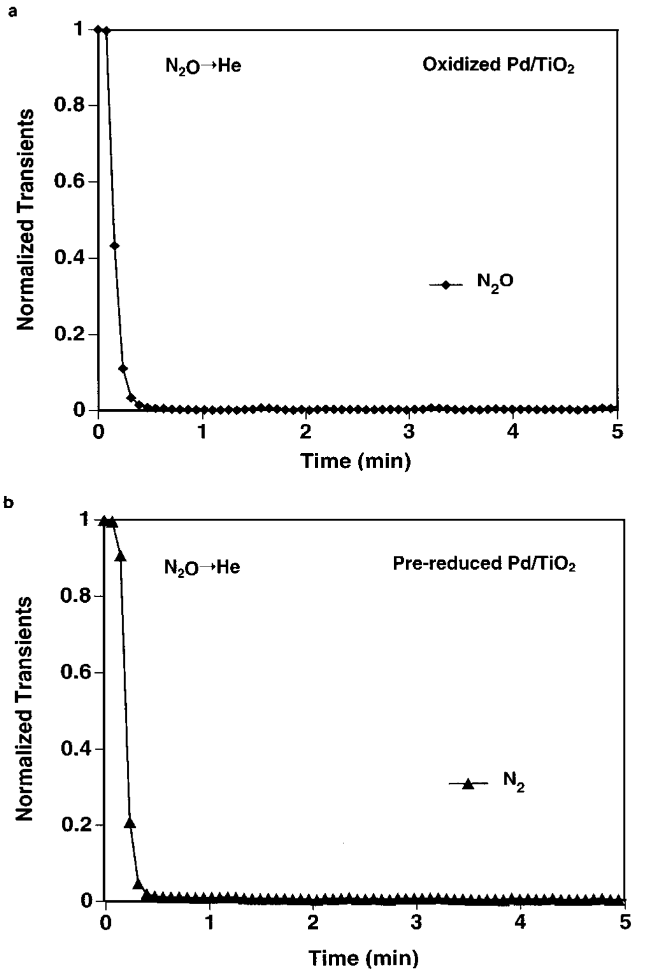

FIG. 10. Normalized transients in $N_2O \rightarrow He$ switch over (a) oxidized Pd/TiO_2 and (b) prereduced Pd/TiO_2.

In order to rule out the possibility that the slow-decaying N_2O transients could be due to a slow desorption of N_2O from the surface, we ran some control experiments where we have switched the feed stream from N_2O to He and monitored the transients. The transients obtained over the oxidized and the prereduced catalysts are presented in Fig. 10. Over the oxidized catalyst, the N_2O signal dropped immediately after the N_2O stream was switched off. Over the prereduced catalyst, there was N_2 formation and its signal also decayed to zero within the gas-phase hold-up time. These control experiments provided evidence that it was not the nitrous oxide itself which was lingering on the surface, but it was a coupled surface intermediate, possibly a dimeric species, that resided on the surface longer.

Interaction of CH_4 with Pd/TiO_2 Surfaces

Methane adsorption and reaction over palladium catalysts has been studied extensively in the literature (35–40). Palladium catalysts are well known for their methane activation capabilities in oxidation reactions. In our temperature-programmed desorption experiments, it was observed that methane can adsorb, both reversibly and dissociatively, on Pd/TiO_2 surfaces (13). The dissociatively adsorbed methane leads to the formation of carbon oxides and water. Decomposition of methane leading to CH_x species has been discussed in detail by Solymosi and co-workers (41, 42).

Although indirectly, we have also seen evidence of the stability of CH_x species on Pd sites through our transient experiments performed using isotopically labeled species. As seen in Figs. 8b and 8c, when methane is abruptly cut off from the feed stream, the transient for CO_2 does not relax to zero in the same time frame as the CO transient (or the inert transient) does. The fact that we continue seeing significant levels of CO_2 coming from the surface long after the methane source is turned off shows that there are carbonaceous species forming on the surface under reaction conditions with feed mixtures of $CH_4 + NO + O_2$ or $CH_4 + NO$ (Figs. 8b and 8c) as well as when the surface is exposed to CH_4 at the reaction temperature (Fig. 8d). The only time the CO_2 transient relaxes to zero at the same rate as the inert is when there is no oxidizing agent left in the system after the switch, as seen in the $CH_4 + NO \rightarrow He$ experiment (Fig. 8a). This result is significant in proving that the delayed relaxation of CO_2 cannot be explained by a slow desorption of this species from the surface. The reason we see such a sharp decline in the CO_2 transient in this experiment is that there is no oxidizing agent left in the system to react with the CH_x species that are on the surface. In order to be able to determine whether what was happening on the surface under reaction conditions was coke deposition or the formation of a stable CH_x species, water transients were monitored in the same set of experiments. The results for four of the step function changes employed, namely $CH_4 + NO \rightarrow NO$, $CH_4 + NO + O_2 \rightarrow NO$, $CH_4 \rightarrow O_2$, and $CH_4 + NO \rightarrow He$, are presented in Fig. 11. Again, we see that the water transients mimic the relaxation behavior exhibited by CO_2 transients, demonstrating that the carbon oxide formation is accompanied by water formation, which is an indirect evidence of the existence of a CH_x species on the surface. The small differences observed between the CO_2 transients and H_2O transients can be explained by the differences in the desorption rates of the two species. The difference in the relaxation rate of the water transient in the $CH_4 + NO \rightarrow He$ versus $CH_4 + NO \rightarrow NO$ switch is significant in showing that the desorption of water several minutes after the CH_4 stream is cut off is not due to a slow desorption rate of the water, but rather is because of the formation of water from the surface CH_x species.

Proposed Reaction Scheme and Mechanistic Aspects

There has been a lot of work reported in the literature regarding the mechanism and intermediates of the

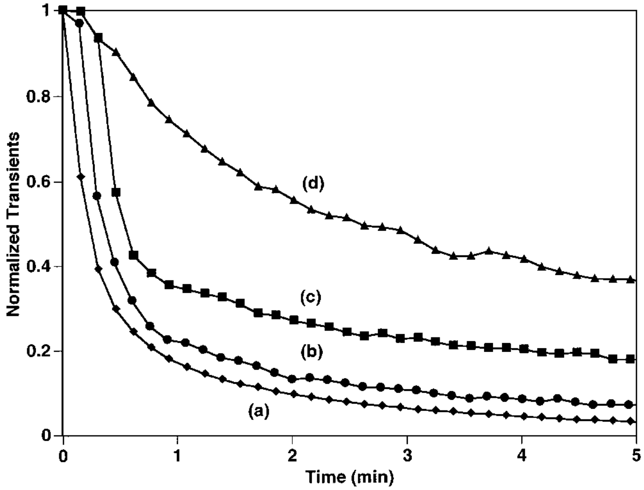

FIG. 11. Normalized transients for H_2O in (a) $^{13}CH_4 + NO \rightarrow He$ switch, in (b) $^{13}CH_4 + NO + O_2 \rightarrow NO$ switch, in (c) $^{13}CH_4 + NO \rightarrow NO$ switch, and in (d) $^{13}CH_4 \rightarrow O_2$ switch.

$NO + CH_4$ reaction. One of the earliest mechanisms proposed for the NO–CH_4 reaction in the absence of oxygen was by Hardee & Hightower (43) over Rh/Al_2O_3. They have suggested that both N_2 and N_2O are primary products in the overall reaction scheme whereas N_2O(ad) could be a surface intermediate in the formation of N_2. Also, the rate-determining step was suggested to involve the breaking of the C–H bond in CH_4. Vannice *et al.* (44, 45) have suggested different mechanisms for this reaction in the presence and in the absence of oxygen over La_2O_3 and Sr/La_2O_3 catalysts (44). In the absence of oxygen they have suggested a N_2O^* intermediate leading to N_2 formation while in the presence of oxygen they have proposed formation of NO_2^* as well as N_2O^* as an intermediate for N_2 formation. Over Li/MgO (45), however, they have argued against the formation of an NO_2^* intermediate in the absence of oxygen. Hall and co-workers have investigated the NO reduction reaction in great detail over ZSM-5 catalysts with several different hydrocarbons as reducing agents and summarized the results in a recent article (46). They have suggested the role of NO_2 to be an intermediate in the formation of N_2. At higher temperatures, they observed a decrease in the NO conversion activity and they explained that the decrease in the formation of NO_2 was due to depletion of O_2 by methane combustion. Li and Armor (8, 9), who have worked on similar catalysts, have suggested that at higher temperatures methane conversion increased, decreasing its availability for NO reduction, and subsequently NO reduction levels were decreased. Over Co–ZSM-5 there was negligible activity observed in the absence of oxygen whereas the activity increased with an increase in O_2 concentration. Based on this, it was suggested that NO_2 was formed through the reaction of NO and O_2 and it then reacted with adsorbed methane to give N_2. Cowan *et al.* (47) have indicated that over the Co–ZSM-5 catalyst the rate-determining step is the breaking of the C–H bond by the adsorbed NO_2 intermediate. Another mechanism proposed in the literature involves direct decomposition of NO to nitrogen and oxygen, with oxygen being consumed to oxidize the surface (11, 12). In these studies, which were conducted over metal-exchanged ZSM-5 catalysts, the role of the hydrocarbon was suggested to be reduction of the catalyst, and hence, regeneration of the active sites. A review of the literature makes it clear that there may be different mechanisms in operation on different catalysts.

In this study, the isotopic labeling experiments under steady state as well as transient conditions have provided some important clues regarding the routes through which N_2 and N_2O are formed. NO and CH_4 were seen to strongly adsorb/interact with the oxidized as well as with the prereduced Pd/TiO_2 surfaces as demonstrated in our earlier TPD experiments (13, 15). Based on our results and other evidence presented in the literature (42, 45), it is envisioned that methane is activated on metallic Pd sites through a dissociation process as follows:

$$CH_{4(g)} \rightarrow CH_{x(s)} + (4 - x)H_{(s)}. \qquad [1]$$

We believe that the resulting CH_x species can reside on the surface for a long time and need an oxidizing agent such as NO or O_2 to desorb. We also propose that these are the species involved in reduction of NO to N_2, possibly through the formation of a methyl-dinitrosyl type surface intermediate. As suggested by the fast declines of labeled nitrogen transients in the step function changes such as $CH_4 + {}^{15}NO + O_2 \rightarrow CH_4 + {}^{14}NO + O_2$ and $CH_4 + {}^{15}NO \rightarrow CH_4 + {}^{14}NO$, this intermediate, which is represented as $[CH_x\text{–}NO\text{–}NO]^*_{(s)}$, appears to have a very short surface life and can decompose readily to give N_2 and CO_2 as follows:

$$[CH_x\text{–}NO\text{–}NO]^*_{(s)} \rightarrow N_2 + CO_2 + xH_{(s)}. \qquad [2]$$

Also, the fact that there was no cross-labeled nitrogen in any of these experiments leads us to propose that it is not two separate nitrosyl groups that lead to N_2 formation, but rather a dinitrosyl-type species. Finally, when we compared the amount of O-16 appearing in carbon dioxide and in nitric oxide after the $CH_4 + {}^{14}N^{16}O \rightarrow CH_4 + {}^{15}N^{18}O$ and ${}^{14}N^{16}O \rightarrow {}^{15}N^{18}O$ switches, respectively, we found that the amount of O-16 in CO_2 in the former switch follows very closely the amount of O-16 seen in nitric acid after the latter switch (Fig. 12). This observation provides further support to the proposed scheme by showing that the oxygen atoms in CO_2 are likely to originate from two NO molecules, which may be brought together in a methyl dinitrosyl-type intermediate.

Based on the observations outlined in this and the previous reports (13, 14), it is also envisioned that N_2O formation takes place without any direct involvement of methane, but

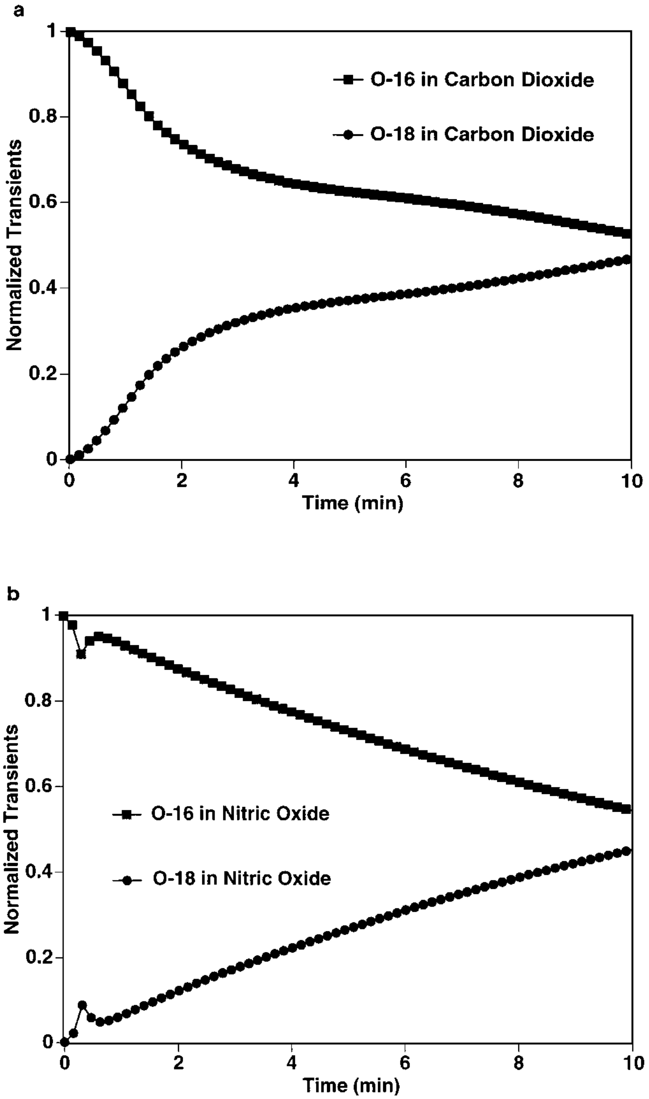

FIG. 12. Normalized O-16 and O-18 transients in (a) carbon dioxide in $CH_4 + {}^{15}N^{16}O \rightarrow CH_4 + {}^{15}N^{18}O$ switch and in (b) nitric oxide in ${}^{14}N^{16}O \rightarrow {}^{15}N^{18}O$ switch.

essentially by the coupling of two NO molecules through a dimeric intermediate. The findings in this study do not provide any information about the nature of these intermediates, i.e., whether they are dimer-type surface species or dinitrosyl groups associated with the palladium sites.

The formation of dimer or dinitrosyl species has been proposed in the literature over several types of surfaces, including zeolites (48), oxides (49), char (50), and noble metals. Noble metal catalysts including Rh (32), Pt (33), and Pd (34) have also been reported as adsorbing NO in dimeric forms over their surfaces. The decomposition of the dimeric species to N_2O has also been reported over various catalysts, including zeolites (48) and supported Ag catalysts (51). Based on the evidence provided by isotopic labeling experiments, we believe the dimer species proposed in this study to be much more stable compared to the methyl–nitrosyl species proposed in Reaction 2. The dimer species is thought to decompose as follows to give a nitrous oxide molecule in the gas phase:

$$(NO)_{2(s)} \rightarrow N_2O_{(g)} + O_{(s)}. \qquad [3]$$

It has been shown that N_2O can form over both palladium oxide and metallic palladium. It is the only product from NO decomposition over PdO. We also suspect that the presence of a CH_x species on the surface inhibits the dimer formation, possibly due to the consumption of the NO through the methyl–dinitrosyl species. However, once the dimers are formed, the presence of gas phase methane or surface CH_x species can possibly aid in the removal of the O atom from the dimeric intermediate and, indirectly, enhance the desorption rate of N_2O desorption. We have seen an evidence of this phenomenon when we compared the N_2O transients following ${}^{13}CH_4 + NO \rightarrow He$ and ${}^{13}CH_4 + NO \rightarrow CH_4$ switches performed over the reduced catalyst (16). We saw N_2O desorption from the surface in both experiments after the switch. However, the desorption of N_2O in the first experiment showed a long delay and was at a much slower rate than it was in the second experiment.

Over the reduced catalyst, NO decomposition (without methane) is shown to produce some nitrogen as well. It has also been shown that N_2O can further decompose to nitrogen over reduced sites. So it is possible that the nitrogen observed in the NO decomposition experiment is a result of further decomposition of the N_2O, which was originally formed through the same type of dimeric intermediate.

The fact that N_2O partially decomposes to N_2 over the reduced catalyst raises the question of whether N_2O could be an intermediate leading to nitrogen in the $NO + CH_4$ reaction as well. If this were the case we would expect to see some delayed relaxation of labeled nitrogen signal in switches such as $CH_4 + {}^{15}NO + O_2 \rightarrow CH_4 + {}^{14}NO + O_2$, $CH_4 + {}^{15}NO_2 \rightarrow CH_4 + {}^{14}NO$, and $CH_4 + {}^{15}NO + O_2 \rightarrow CH_4 + O_2$. Since the labeled nitrogen transient always decays to zero within the gas-phase hold-up time, we are ruling out this possibility as a major reaction route.

Although NO_2 is suggested as a possible intermediate in the NO/CH_4 reaction in the literature, all of these studies have reported essentially no activity in the absence of oxygen. The fact that we had very high NO reduction activity in the absence of oxygen argues against NO_2 being a primary intermediate in the reaction network over the Pd/TiO_2 catalyst. Similar findings have been reported in the literature about high NO reduction activity in the absence of O_2 over several rare earth oxides (45) and over Pd/ZSM-5 catalysts (12), pointing out that the reaction schemes are quite specific to the catalysts used.

In addition to the CH_x–NO interaction and direct NO decomposition, a third reaction that is in operation in this system is direct combustion of methane, which is likely to be favored over the oxidic palladium sites. We envision that the direct combustion of methane on PdO sites leads to the formation of CO, which could oxidize further to CO_2 if there is sufficient oxygen available.

In the next article in this series, we will present a more detailed analysis of the conditions which dictate the phase transformations of the catalyst and the resulting changes in its catalytic functionality (52).

ACKNOWLEDGMENTS

The financial support provided for this work from National Science Foundation through Grant CTS- 9412544 and from the Exxon Foundation is gratefully acknowledged.

REFERENCES

1. Iwamoto, M., Furukawa, H., Mine, Y., Uemura, F., Mikuriya, S., and Shuichi, K., *J. Chem. Soc. Chem. Comm.*, 1272 (1986).
2. Kharas, K. C. C., Robota, H. J., and Liu, D. J., *Appl. Catal. B: Environ.* **2**, 225 (1993).
3. Ukisu, Y., Sato, S., Abe, A., and Yoshida, K., *Appl. Catal. B: Environ.* **2**, 147 (1993).
4. Hamada, H., Kintaichi, Y., Sasaki, M., Ito, T., and Tabata, M., *Appl. Catal.* **64**, L1 (1990).
5. Bethke, K. A., Li, C., Kung, M. C., Yang, B., and Kung, H. H., *Catal. Lett.* **31**, 287 (1995).
6. Feeley, J. S., Deeba, M., Farrauto, R. J., Beri, G., and Haynes, A., *Appl. Catal. B: Environ.* **6**, 79 (1995).
7. Misono, M., and Kondo, K., *Chem. Lett.*, 1001 (1991).
8. Li, Y., and Armor, J. N., *Appl. Catal. B: Environ.* **2**, 239 (1993).
9. Li, Y., and Armor, J. N., *J. Catal.* **150**, 376 (1994).
10. Zhang, X., Walters, A. B., and Vannice, M. A., *J. Catal.* **155**, 290 (1995).
11. Loughran, C. J., and Resasco, D. E., *Appl. Catal. B: Environ.* **5**, 351 (1995).
12. Burch, R., and Scire, S., *Appl. Catal. B: Environ.* **3**, 295 (1994).
13. Ozkan, U. S., Kumthekar, M. W., and Karakas, G., *Catal. Today*, accepted for publication.
14. Kumthekar, M. W., and Ozkan, U. S., *J. Catal.* **171**, 45 (1997).
15. Kumthekar, M. W., and Ozkan, U. S., *Catal. Today* **35**, 107 (1997).
16. Kumthekar, M. W., and Ozkan, U. S., *Appl. Catal. A: General* **151**(1), 289 (1997).
17. Janssen, F. J. J. G., Kerkhof, M. G., Bosch, H., and Ross, J. R. H., *J. Phys. Chem.* **91**, 5921 (1987).
18. Janssen, F. J. J. G., Kerkhof, M. G., Bosch, H., and Ross, J. R. H., *J. Phys. Chem.* **91**, 6633 (1987).
19. Duffy, B. L., Curry-Hyde, H. E., Cant, N. W., and Nelson, P. F., *J. Catal.* **154**, 107 (1995).
20. Driscoll, S. A., and Ozkan, U. S., *J. Phys. Chem.* **97**, 11524 (1993).
21. Driscoll, S. A., Gardner, D. K., and Ozkan, U. S., *Catal. Lett.* **25**, 191 (1994).
22. Ozkan, U. S., Cai, Y., and Kumthekar, M. W., *J. Catal.* **149**, 374 (1994).
23. Ozkan, U. S., Cai, Y., and Kumthekar, M. W., *J. Catal.* **149**, 390 (1994).
24. Gesser, H. D., and Kruczynski, L., *J. Phys. Chem.* **88**, 2751 (1984).
25. Hulzinga, T., and Prins, R., *J. Phys. Chem.* **85**, 2156 (1981).
26. DeCanio, S. J., Apple, T. M., and Dybowski, C. R., *J. Phys. Chem.* **87**, 194 (1983).
27. Conesa, J. C., and Soria, J., *J. Phys. Chem.* **86**, 1392 (1982).
28. Winter, E. R. S., *J. Chem. Soc. Ser. A*, 2889 (1969).
29. Shelef, M., *Catal. Rev.-Sci. Eng.* **11**(1), 1 (1975).
30. Ozkan, U. S., Cai, Y., and Kumthekar, M. W., *J. Phys. Chem.* **99**(8), 2363 (1995).
31. Ozkan, U. S., Kumthekar, M. W., and Cai, Y., *Ind. Eng. Chem. Res.* **33**(12), 2924 (1994).
32. Liang, J., Wang, H. P., and Spicer, L. D., *J. Phys. Chem.* **89**, 5840 (1985).
33. Yoshinobu, J., and Kawai, M., *Chem. Lett.*, 605 (1995).
34. Nyberg, C., and Uvdal, P., *Surf. Sci.* **204**, 517 (1988).
35. Baldwin, T. R., and Burch, R., *Appl. Catal.* **66**, 337 (1990).
36. Seimanides, S., and Stiukides, M., *J. Catal.* **98**, 540 (1986).
37. Hicks, R. F., Qi, H., Young, L., and Lee, R. G., *J. Catal.* **122**, 280 (1990).
38. Oh, S. E., Mitchell, P. J., and Siewart, R. M., *J. Catal.* **132**, 287 (1991).
39. Schmidt, L. D., and Huff, M., *Catal. Today* **21**, 443 (1994).
40. Burch, R., and Loader, P. K., *Appl. Catal. B: Environ.* **5**, 149 (1994).
41. Solymosi, F., Erdohelyi, A., Cserenyi, J., and Felvegi, A., *J. Catal.* **147**, 272 (1994).
42. Solymosi, F., *Catal. Today* **28**, 193 (1996).
43. Hardee, J. R., and Hightower, J. W., *J. Catal.* **86**, 137 (1984).
44. Vannice, M. A., Walters, A. B., and Zhang, X., *J. Catal.* **159**, 119 (1996).
45. Zhang, X., Walters, A. B., and Vannice, M. A., *J. Catal.* **146**, 568 (1994).
46. Witzel, F., Sill, G. A., and Hall, W. K., *J. Catal.* **149**, 229 (1994).
47. Cowan, A. D., Dumpelmann, R., and Cant, N. W., *J. Catal.* **151**, 356 (1995).
48. Aylor, A. W., Larsen, S. C., Reimer, J. A., and Bell, A. T., *J. Catal.* **157**, 592 (1995).
49. Rethwisch, D. G., and Dumesic, J. A., *J. Phys. Chem.* **90**, 1625 (1986).
50. Teng, H., and Suuberg, M., *J. Phys. Chem.* **91**, 478 (1993).
51. Brown, W. A., Gardner, P., and King, D. A., *J. Phys. Chem.* **99**, 7065 (1995).
52. Ozkan, U. S., Kumthekar, M. W., and Karakas, G., *J. Catal.* **171**, 67 (1997).